# New Light on Some Old Problems: Revisiting the Stefan Tube, Graham's Law, and the Bosanquet Equation

**Piet J. A. M. Kerkhof**[†]

*Laboratory for Separation Processes and Transport Phenomena, Faculty of Chemical Engineering and Chemistry, Eindhoven University of Technology, P.O. Box 513, 5600 MB Eindhoven, The Netherlands*

The Stefan diffusion tube is modeled with the recently developed binary friction model (BFM), and it is shown that this model can describe all kinds of vapor flow regimes from Stefan diffusion to pure pressure-driven flow but also Knudsen and (diffusive) slip flow. From the BFM simple criteria are derived for the transition between various regions, the criteria of which are also relevant to the fields of gas adsorption, heterogeneous catalysis, and drying of porous materials. For isobaric counterdiffusion the BFM shows where the limits of Graham's law are. For equimolar counterdiffusion analogously the area of applicability of the Bosanquet equation is derived from the BFM and an extended equation is given.

## 1. Introduction

In 1994 Professor Stephen Whitaker held a seminar at our laboratory and stated: "It took me a long time to understand the problem of the Stefan Tube, so I wrote three papers about it". In these papers (Whitaker, 1988, 1989, 1991), he focused attention on the discrepancy in thinking about the flow of one component, say water vapor, in a tube in which another component, say air, is effectively stagnant. When confronted with a picture like that in Figure 1a, most students as well as teachers approach the problem as one of binary molecular diffusion, along the lines of Bird et al. (1960), and thus implicitly assume a flat radial concentration profile. In the consideration of the transport of the vapor from a boiling liquid, as depicted in Figure 1b, the same people are more or less conditioned to primarily regard the hydrodynamics and solve the Navier−Stokes equation for sufficiently small Reynolds numbers to obtain the parabolic Poiseuille velocity profile. From the species momentum equation Whitaker showed that the diffusion equation over a very wide range very closely approaches the more general momentum balances, and he derived a criterion for this range which will be considered later. He also pointed out the situation of Figure 1c, stating that "while virtually *all* chemical engineers can solve the situation for Figure 1a, virtually none can solve the problem of Figure 1c". I have added here the more or less equivalent system of Figure 1d, in which we have a porous plug. Quite a few chemical engineers remember their training in chemical reaction engineering and state that Graham's law should apply.

In research areas like drying of porous materials, heterogeneous catalysis, membrane ultrafiltration, and adsorption, considerations on the (meso- and macro-) pore level very often are formulated in terms of fluxes and driving forces without explicitly formulating the fact that radial differences in species velocities are present. From the viewpoint of chemical engineering modeling the use of cross-sectional averaged fluxes makes sense since it keeps the already complicated models within both conceptual and computational bounds. For a simple model element such as a cylindrical pore, one would therefore like to have expressions of the averaged fluxes in terms of concentration or partial pressure gradients. It is also interesting to observe that for the different fields mentioned different concepts are commonly used: for drying the vapor transport is treated as Stefan diffusion (Krischer and Kast, 1978); in ultrafiltration individual friction coefficients are considered (Lightfoot, 1974; Robertson and Zydney, 1988); in catalysis and adsorption the dusty gas model (Mason and Malinauskas, 1983; Jackson, 1977) and the Bosanquet equation are used for the transport in the meso- and macropores (Froment and Bischoff, 1979; Kärger and Ruthven, 1992).

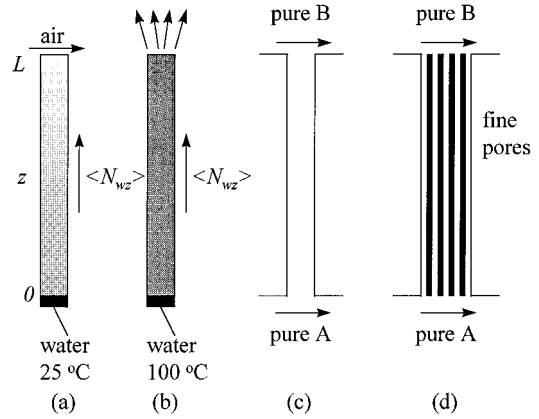


**Figure 1.** Schematic presentation of various capillary and pore transport problems: (a) diffusion of water vapor through stagnant air in the Stefan tube; (b) pressure-driven flow of water vapor through a tube; (c) counterdiffusion of two species through a tube; (d) counterdiffusion of two species through a porous plug.

Although Whitaker meticulously presents the assumptions and restrictions under which the diffusion equation closely approaches the species momentum equations, no general solution in closed form is available for these equations. For engineering and educational purposes it is of interest to have an expression for the flux which could cover both the situation of molecular diffusion and that of laminar flow. With reference to the more microscopic phenomena indicated, it would even be more preferable to have an expression which also could cover the slip and Knudsen flow regions. In his considerations Whitaker limited himself to the region in which the capillary radius was large with respect to the mean free path of the molecules. This is a necessary condition for the use of continuum models as obtained from kinetic gas theory, since no wall effects are enclosed in the integrations associated with the approximate solutions of the Boltzmann equations. Several authors have approached the wall effects from statistical mechanics, starting with Maxwell (1879) and

[†] Telephone: +31-40-2472973. Fax: +31-40-2446104. E-mail: tgtcpk2@chem.tue.nl.

S0888-5885(96)00542-8 CCC: $14.00 

Kramers and Kistemaker (1943). More advanced and accurate work on these diffusive slip phenomena or baroeffect has been presented by a large number of authors, e.g., Lang and Loyalka (1970) and Noever (1990). Recently, also two-dimensional studies by means of molecular dynamics and Monte Carlo methods have been presented, e.g., Mo and Rozenberger (1991) and Cergignani and Sharipov (1992). For chemical engineering purposes both the statistical mechanics and the numerical approaches have the disadvantage that they do not lead to tractable equations with easily identifiable parameters, even for the most simple situations such as binary diffusion in a capillary.

In recent work which started from membrane ultrafiltration I extended the Lightfoot friction model (Lightfoot, 1974) into a new model, the binary friction model, which relates pore-averaged fluxes to driving forces, introducing friction coefficients related to individual viscosity contributions (Kerkhof, 1996). The model gives remarkably good coverage of both ultrafiltration of aqueous poly(ethylene glycol) solutions and several gas diffusion phenomena such as the counterdiffusion of He and Ar across porous graphite plugs (Evans et al., 1962, 1963) and counterdiffusion of various gases in capillaries (Waldmann and Schmitt, 1961). In the process I discovered errors in the basic derivations of the dusty gas model of Mason et al. (1967, 1978, 1983, 1985, 1990), which had been used to explain counterdiffusion phenomena and still finds widespread application, and also in heterogeneous catalysis (Jackson, 1977; Froment and Bischoff, 1979; Veldsink et al., 1995; Keil, 1996) and adsorption (Kärger and Ruthven, 1992). One of the conclusions from the analysis is that the picture of a simultaneous viscous and diffusive flux of Mason et al., in some regions also paralled by a Knudsen flux, is inherently incorrect and should be replaced by the proper addition of friction forces.

In the next sections the binary friction model will first be worked out for the situation of the Stefan tube, and from it criteria for various limiting regimes will be derived. The same type of considerations will be used to derive general equations for isobaric diffusion, from which the limits of application of Graham's law follow. Also for the case of equimolar countertransport an effective diffusion coefficient is derived, and a criterion is given under which this goes over in the Bosanquet equation.

## 2. Binary Friction Model (BFM) for Isothermal Gas Transport in a Capillary

The binary friction model relates pore-cross-section-averaged fluxes with pore-cross-section-averaged driving forces, with nonadsorbing walls. Since in the radial direction $r$ certainly a gradient in the component velocities in the axial $z$-direction may be expected and also partial pressure gradients may occur in the $r$-direction, we will use the following notation:

$$\langle P_i \rangle = \frac{1}{A}\int_A P_i \, \mathrm{d}A$$

$$\langle N_{iz} \rangle = \frac{1}{A}\int_A N_{iz} \, \mathrm{d}A \qquad (1)$$

in which it is recognized that in the cross-section averaging we only retain the axial $z$-component of the flux. These definitions are emphasized here because of the confusion in many papers between local and cross-section-averaged scalars and fluxes. It will be assumed, however, that the radial gradient in the total pressure can be neglected and so for this we use the notation $P_t$. Also for flow of a single gas g, we will assume negligible radial pressure gradients and use the notation $P_g$. For the magnitude of the averaged flux vector $\langle N_{iz} \rangle$, we will use $|\langle N_{iz} \rangle|$.

For isothermal transport of gases in a capillary the binary friction model (BFM) reads in the absence of electrical, magnetical, and gravitational fields (Kerkhof, 1996):

$$\left.\frac{\partial \langle P_i \rangle}{\partial z}\right|_T = RT\sum_{j=1}^{n}\frac{\Phi_{ij}(x_i\langle N_{jz}\rangle - x_j\langle N_{iz}\rangle)}{P_t \text{Đ}_{ij}} - f_{im}RT\langle N_{iz}\rangle \qquad (2)$$

in which the left-hand side represents the driving force in terms of the gradient in chemical potential, the first term on the right-hand side the interspecies friction, and the last term the friction between species $i$ and the wall. The fluxes are averaged over the pore cross section. The factor $\Phi_{ij}$ was formally introduced to allow for disappearance of the interspecies friction at the zero-pressure limit. However, for a large number of practical cases considered, it turned out that good agreement between theory and experiment was obtained for $\Phi_{ij} = 1$, and thus we may write eq 2 somewhat simpler as:

$$\left.\frac{\partial \langle P_i \rangle}{\partial z}\right|_T = RT\sum_{j=1}^{n}\frac{(x_i\langle N_{jz}\rangle - x_j\langle N_{iz}\rangle)}{P_t \text{Đ}_{ij}} - f_{im}RT\langle N_{iz}\rangle \qquad (3)$$

The friction coefficient with the wall is given by:

$$f_{im} = \left(D_i^K + \frac{B_0}{\kappa_i}\right)^{-1} \qquad (4)$$

in which $D_i^K$ is an effective Knudsen coefficient and $B_0$ is the permeability, which for a capillary is equal to:

$$B_0 = {r_0}^2/8 \qquad (5)$$

Approaching the slip flow region for a single gas g with a linear two-term Maxwell equation (Maxwell, 1879; Kerkhof, 1996):

$$|\langle N_{gz}\rangle| = -\left(\frac{{r_0}^2}{8\eta}\frac{P_{g0}+P_{gL}}{2} + D_g^K\right)\frac{1}{RT}\frac{P_{g0}-P_{gL}}{L} \qquad (6)$$

and thus neglecting the small curvature found by Knudsen, the effective Knudsen coefficient is equal to:

$$D^K \approx 0.89 D_0^K \qquad (7)$$

Here $D_0^K$ is the zero-pressure Knudsen diffusion coefficient:

$$D_{g0}^K = \frac{2}{3}r_0\left(\frac{8RT}{\pi M_g}\right)^{1/2} \qquad (8)$$

The coefficient $\kappa_i$ in eq 4 represents the fractional viscous contribution to the overall friction between component $i$ and the wall, thus replacing the viscosity $\eta$ in the single-gas equation 6. For a gaseous mixture holds:

$$\sum_{i=1}^{n}\kappa_i x_i = \frac{\eta}{P_t} \qquad (9)$$

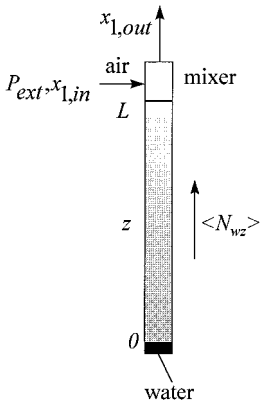


**Figure 2.** Schematic view of the Stefan tube equipped with mixer with outside air at the outlet which allows for "fluitketel"-boundary condition.

From the Chapman−Enskog theory follows (Reid et al., 1977):

$$\eta = \sum_{i=1}^{n} \frac{x_i \eta_i^\circ}{\sum_{j=1}^{n} x_j \xi_{ij}} \tag{10}$$

in which $\eta_i^\circ$ are the pure-component viscosities and $\xi_{ij}$ are the Wilke parameters:

$$\xi_{ij} = \frac{[1 + (\eta_i^\circ/\eta_j^\circ)^{1/2}(M_j/M_i)^{1/4}]^2}{[8(1 + M_i/M_j)]^{1/2}} \tag{11}$$

This gives for the $\kappa$:

$$\kappa_i = \frac{1}{P_t} \frac{\eta_i^\circ}{\sum_{j=1}^{n} x_j \xi_{ij}} \tag{12}$$

Let us now consider the Stefan tube with the evaporating liquid as component 1 and the stagnant gas as component 2. We thus assume that the gas does not dissolve into the liquid, and thus:

$$|\langle N_{2z}\rangle| = 0 \tag{13}$$

Writing out eq 3 then gives

$$\frac{\partial\langle P_1\rangle}{\partial z} = -RT\frac{1}{P_t \mathcal{D}_{12}}\langle P_2\rangle\langle N_{1z}\rangle - f_{1m}RT\langle N_{1z}\rangle$$

$$\frac{\partial\langle P_2\rangle}{\partial z} = RT\frac{1}{P_t \mathcal{D}_{12}}\langle P_2\rangle\langle N_{1z}\rangle \tag{14}$$

In order to cover all kinds of situations, we consider the total pressure as variable along the length of the capillary.

## 3. Binary Friction Model Applied to the Stefan Tube

First, let the Stefan tube be defined by some simplified assumptions, illustrated by Figure 2. We have a capillary, in which at $z = 0$ we have a stationary evaporating liquid, say water. At $z = L$ we have chosen a somewhat different boundary condition than is usually made in textbooks. From everyday practice we know that, upon cooking a kettle of water, comparable to situation (1b), the outgoing stream from the whistle flows jetlike into the air, and air is sucked into it, leading over some distance to dilution (and condensation). From personal manual observation I found (a very long time ago) that at the exit point of the whistle the gas composition was highly aqueous (and hot!). Therefore, we can, in general, not state that the humidity at $z = L$ is equal to that of the surrounding gas in which the stream exits. A simple model is to let the outgoing stream from the capillary flow into an ideally mixed volume, where it is mixed with the surrounding gas. A mass balance over this mixer gives for steady state:

$$x_{1,out} = \frac{x_{1,in} + |\langle N_{1z}\rangle|A_{capp}/\phi_{air}}{1 + |\langle N_{1z}\rangle|A_{capp}/\phi_{air}} \tag{15}$$

In view of its origin we shall call this the "fluitketel"-boundary condition, which holds at $z = L$. The system was solved for $H_2O-N_2$ numerically as follows for $x_{1,in} = 0$ and $\phi_{air} = 0.01 d_{capp}^2 C_{tL}$. The capillary temperature was taken to be equal to the liquid water temperature. In first attempts the water temperature was chosen as an independent variable, and the fluxes were integrated numerically. However, for not too small capillaries in the region near the boiling point enormous changes in the water flux occurred over a very small temperature range. In order to view the behavior over a large range, the water flux was chosen as the independent variable, and the water temperature at $z = 0$ was evaluated in an iterative way. First, the temperature was estimated. Subsequently, all coefficients were evaluated at that temperature.

The equation for the stagnant component gives upon integration:

$$\ln\left(\frac{\langle P_{2,L}\rangle}{\langle P_{2,z}\rangle}\right) = \frac{RT}{P_t \mathcal{D}_{12}}(L - z) \tag{16}$$

in which it is recognized that the diffusion coefficient may vary with the total pressure over the capillary length, but the product $P_t\mathcal{D}_{12}$ remains constant. The water pressure gradient was then integrated over the capillary length, starting from the top. This again gives the corrected vapor pressure at the bottom, from which a new temperature estimate follows. Five iterations were sufficient in all cases to obtain convergence.

In order to compare the results, the following limiting cases were also evaluated.

**Stefan Diffusion.**

$$|\langle N_{1z}\rangle| = -\frac{P_t}{RT}\mathcal{D}_{12}\ln\left(\frac{P_t - \langle P_{1L}\rangle}{P_t - \langle P_{10}\rangle}\right) \tag{17}$$

This expression was evaluated with $P_t = P_{ext}$, for the region in which the vapor pressure at $z = 0$ lower than the external total pressure.

**Viscous Flow.** This was depicted as the flow of pure water vapor without stagnant gas:

$$|\langle N_{1z}\rangle| = \frac{B_0}{RT\eta_1^\circ L}\frac{(P_{10} + P_{1L})}{2}(P_{10} - P_{1L}) \tag{18}$$

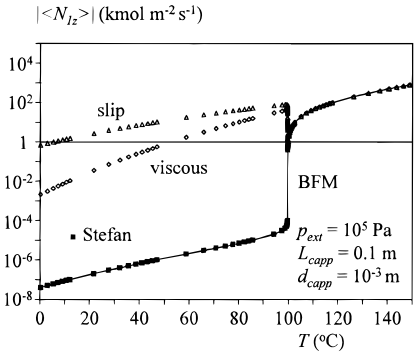


**Figure 3.** Water flux dependent on liquid water temperature according to the binary friction model (BFM) and various other approximations for a capillary of 1 mm diameter at 1 bar external pressure.

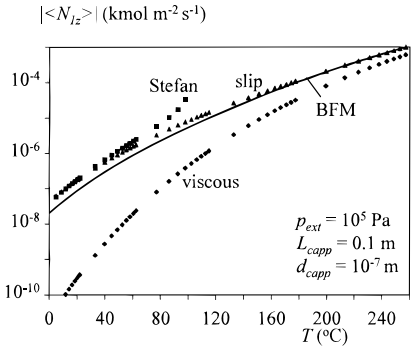


**Figure 4.** Water flux dependent on liquid water temperature according to the binary friction model (BFM) and various other approximations for a capillary of 0.1 $\mu$m diameter at 1 bar external pressure.

**Slip Flow.** Here again the pure gas flow without hindrance from the stagnant gas is considered, and so we have from eq 6:

$$|\langle N_1 \rangle| = \left( \frac{B_0}{\eta_1^\circ} \frac{(P_{10} + P_{1L})}{2} + D_1^K \right) \frac{1}{RT} \frac{(P_{10} - P_{1L})}{L} \quad (19)$$

The first case considered was that of a 1 mm capillary diameter at atmospheric outside pressure, and the results are shown in Figure 3. Over a large temperature range the Stefan equation coincides with the binary friction model results, virtually up to 100 °C. In this region below the boiling point it is clear that the expressions for the viscous flux and slip flow give way too high predictions. Near the boiling point the fluxes from these expressions fall down, because of the higher vapor pressure in the "whistle", thus decreasing the difference in vapor pressure over the tube. Above the boiling point both slip flow and viscous flow essentially give the same results, since with the 1 mm radius and atmospheric pressure Knudsen flow does not play a significant role. The higher value of the slip flow predictions at low temperatures disappears above the boiling point because of the large increase in $\langle P_1 \rangle$ over the whole length of the tube.

A second case was that of a 0.1 $\mu$m diameter, again at atmospheric pressure. The results are presented in Figure 4. It shows in the first place that even at low temperatures the Stefan equation does not cover the results of the binary friction model. The explanation is that wall friction effects cannot be neglected with respect to interspecies friction, as was allowed for the larger capillary. The slip flow results are too high at low temperatures but at higher temperatures coincide

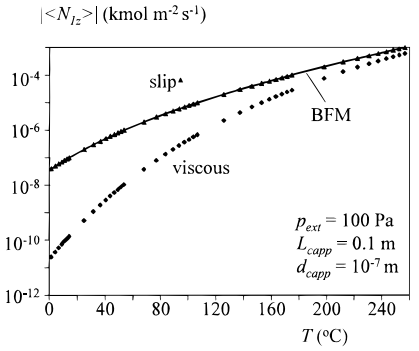


**Figure 5.** Water flux dependent on liquid water temperature according to the binary friction model (BFM) and various other approximations for a capillary of 0.1 $\mu$m at 100 Pa external pressure.

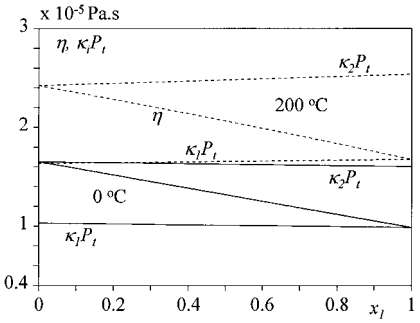


**Figure 6.** Specific fractional viscosity coefficients $\kappa$ and mixture viscosities for the system water (1)−nitrogen (2), as dependent on composition and temperature.

with those of the binary friction model, indicating that at lower temperatures the presence of the stagnant gas gives rise to considerable interspecies friction, while at higher temperatures the partial pressure of the stagnant component becomes so low that nearly pure vapor flow is obtained. The results of viscous flow are much lower than those of the BFM, indicating that for pure vapor Knudsen flow is the dominant mechanism.

The third case studied is again for a 0.1 $\mu$m diameter, but now at a low total pressure of 100 Pa, as shown in Figure 5. Here Stefan diffusion no longer occurs, since the total pressure is lower than the vapor pressure over the range considered, and we have a very high mole fraction of vapor, causing the slip flow to coincide with the BFM results.

From these examples it can be concluded that the BFM gives a nice transition between totally different regimes and, as such, could be of educational value in the sense of Whitaker.

## 4. Limiting Regime Considerations from Simple Dimensionless Numbers

In Figure 6 the individual fractional viscosities $\kappa_i$ of water (1) and nitrogen (2) are presented together with the mixture viscosity as dependent on composition for two temperatures. It is clear that there is a strong dependence on temperature, but for $\kappa_i$ only a very weak one on composition. Thus at a given temperature a quite good approximation could be:

$$\kappa_i \approx \eta_i^\circ / P_t \quad (20)$$

In order to address the relative importance of wall friction compared to interspecies friction, I define the following dimensionless expression:

$$Ke_1 = \frac{\text{wall friction force}}{\text{intermolecular friction force}} \qquad (21)$$

From eq 14 it follows that for the present situation this can be written as:

$$Ke_1 = \frac{f_{1m} P_t Đ_{12}}{P_2} = \frac{(P_t Đ_{12})}{\left(D_1^K + \frac{B_0}{\kappa_1}\right) P_t (1 - x_1)} \qquad (22)$$

A high value of $Ke_1$ implies that wall friction is dominating and a low value that intermolecular friction is the most important momentum transfer. Keeping in mind that the product $P_t Đ_{12}$ is independent of pressure, it follows quite straightforwardly that the transport is wall-friction-dominated at low total pressures, at high mole fractions of the transported component $x_1 \rightarrow 1$, and for a given pressure at low values of the capillary radius $r_0$ corresponding to a low value of the permeability $B_0$. In Figure 7 the change in $Ke_1$ for water vapor is shown for an intermediate composition dependent on the capillary radius, with the total pressure as the parameter. At each pressure it follows that at a very small radius the wall friction is dominating, while for large capillaries at sufficiently high pressures the Stefan situation is encountered. More specifically, one can also see that for pores of 1 $\mu$m and smaller wall friction effects cannot be neglected even at atmospheric pressures, and thus in drying this should be taken into account instead of using the Stefan equation. This holds even stronger in the case of vacuum drying. In Figure 8 the effect of composition is given at atmospheric pressure, and it is clear that depending on composition one may change from the Stefan regime into the wall-friction regime. This is illustrated with the dotted line for a pore radius of 0.3 $\mu$m. In the case of a strong composition gradient along the length of the pore, the system may thus change from one regime to the other over the pore length.

Of course, similar diagrams can be drawn for other temperatures, shifting the lines upward with increasing temperature.

Within the wall-friction regime a distinction can be made between the Knudsen and the viscous subregimes. A good measure for this also logically follows from eq 4 as:

$$Ke_2 = \frac{\text{Knudsen friction forces}}{\text{viscous friction forces}} = \frac{D_1^K \kappa_1}{B_0} \qquad (23)$$

A high value of $Ke_2$ implies that Knudsen flow is the dominating mechanism, a low value that viscous friction dominates, and at intermediate values that slip flow dominates, all this under the condition that the flow is wall-friction dominated. The number $Ke_2$ resembles the dimensionless number of Di Napoli et al. (see Froment and Bischoff, 1979):

$$N_{\mathrm{DiN}} = \frac{B_0 P_t}{\eta D_1^K} \qquad (24)$$

However, the difference lies in the specific viscosity coefficient $\kappa$ which occurs in the $Ke_2$ number vs the mixture viscosity in $N_{\mathrm{DiN}}$. In a mixture with a wide range in molecular mass the $Ke_2$ number is therefore more component-specific.

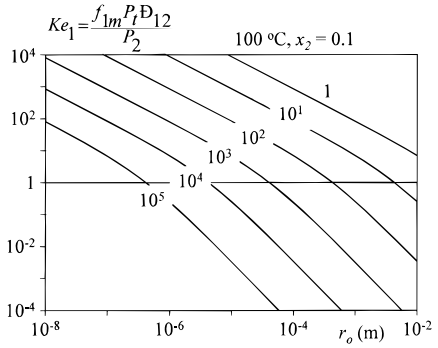


**Figure 7.** Dimensionless $Ke_1$ number for water vapor in the system water (1)−nitrogen (2) dependent on capillary radius, at different total pressures.

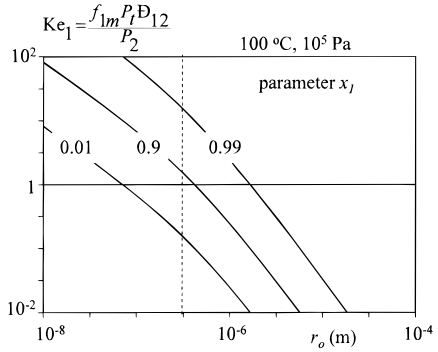


**Figure 8.** Dimensionless $Ke_1$ number for water vapor in the system water (1)−nitrogen (2) dependent on capillary radius, at a total pressure of 1 bar for three different compositions.

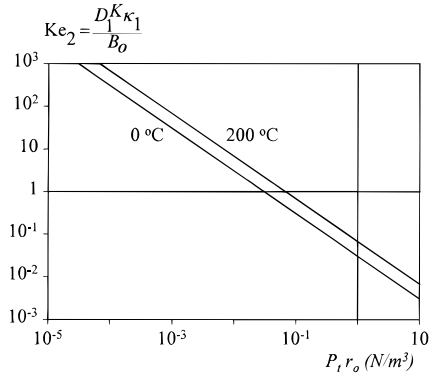


**Figure 9.** Dimensionless $Ke_2$ number for water vapor in the system water (1)−nitrogen (2) dependent on the product of capillary radius and the total pressure for two temperatures.

In Figure 9 this ratio is plotted against the product $P_t r_0$ for two temperatures, since from the basic equations (7), (8), and (20) it follows that at a given temperature:

$$Ke_2 \approx \frac{16}{3} 0.89 \left(\frac{8RT}{\pi M_1}\right)^{1/2} \eta_1 \circ \frac{1}{P_t r_0} \qquad (25)$$

With the combination of Figures 7−9 a very rapid estimation can be made. As an example, the atmospheric transport of water vapor in a pore of 10 nm radius at 10 mol % water and 100 °C is considered. From Figure 7 the first $Ke$ number is read to be nearly 100, and thus the system is in the wall-friction region. With $P_t r_0 = 10^{-3}$ N/m$^3$ for the second number is found $Ke_2 \approx 40$, and so Knudsen flow is the prevailing mechanism. For 99 mol % water, atmospheric pressure, and a pore radius of 0.3 $\mu$m, it follows from Figure 8 that the wall-friction dominates, and from Figure 9 at $P_t r_0 = 3 \times 10^{-2}$ a value of $Ke_2 \approx 1$ is found, indicating slip flow.

Whitaker (1991) derived from the species momentum equations an approximate criterion for which Stefan diffusion could be regarded to occur:

$$Wh = \frac{\eta_{mix}\mathfrak{D}_{12}}{P_t(2r_0)^2(1 - x_1)} \ll 1 \qquad (26)$$

It can be seen that this is a limit of the more general $Ke_1$ criterion, for the case that $Ke_2 < 10^{-2}$, or approximately $P_t r_0 > 1$. Since in his treatment only low Knudsen numbers were considered, the cases of small pores cannot be covered by his criterion.

According to the idea of Knudsen flow, the intermolecular collisions are far less than the molecule−wall collisions, and thus the pressure gradient of the stagnant component should approach zero. In the present formulation it follows at all pressures that:

$$\frac{1}{\langle P_2\rangle}\frac{\partial\langle P_2\rangle}{\partial z} = \frac{RT}{P_t\mathfrak{D}_{12}}\langle N_{1z}\rangle \qquad (27)$$

This implies that there would still be some intermolecular friction; however, at low pressures the flux of 1 also becomes low, leading to only small-pressure gradients of component 2. From an engineering point of view this may be sufficient. It can also be argued that there will always be at least some intermolecular friction, which at very high *Kn* values will not influence the transport of the moving component appreciably but will have a (very small) effect on the distribution of the stagnant gas. An interesting area of research would be to investigate this region in more detail and clarify whether in the general formulation the formal function $\Phi_{12}$ should be involved, which forces the intermolecular term toward zero, and, if so, which form this should take.

## 5. Some Comments on Graham's Law

Graham formulated his "law of effusion" for the fluxes through a porous plug with a pure component on each side, at equal pressures (see Mason and Malinauskas, 1983; Froment and Bischoff, 1979). His results, expressed as the macroscopic plug-cross-section-averaged fluxes, retain the same form in terms of pore-cross-section-averaged flux ratio:

$$|\langle N_{1z}\rangle|/|\langle N_{2z}\rangle| = -(M_2/M_1)^{1/2} \qquad (28)$$

since the effects of porosity and tortuosity cancel out in the flux ratio.

For the Knudsen region this follows directly, but the data for the system He−Ar of Evans et al. (1962), which are more in the slip-flow region, show the same behavior at constant pressure diffusion. Although not convinced of the exact nature of the dusty gas model (Jackson, 1977, p 16), Jackson derives from these equations that Graham's law should hold also at low Knudsen numbers, as for the isobaric case the viscous flow term vanishes and only the terms with the Knudsen coefficients remain, and subsequently derives a multicomponent version of Graham's law (Jackson, 1977, pp 53 and 54). Even stronger, in the description of "the conditions which must be satisfied by any acceptable model for the gasous phase fluxes in a porous medium", his third condition is "condition (iii). For isobaric diffusion in a binary mixture the flux vectors of the two species must satisfy Graham's relation." (Jackson, 1977, pp 65 and 66). For the binary isobaric diffusion the binary friction model reads

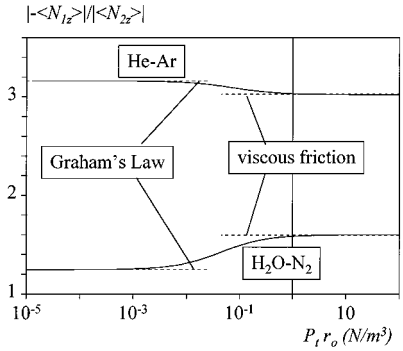


**Figure 10.** Flux ratio at isobaric diffusion for the systems $H_2O-N_2$ and He−Ar, dependent on the product of capillary radius and the total pressure for 298.15 K.

$$\left.\frac{\partial\langle P_1\rangle}{\partial z}\right|_T = RT\frac{(x_1\langle N_{2z}\rangle - x_2\langle N_{1z}\rangle)}{P_t\mathfrak{D}_{12}} - f_{1m}RT\langle N_{1z}\rangle \qquad (29)$$

$$\left.\frac{\partial\langle P_2\rangle}{\partial z}\right|_T = RT\frac{(x_1\langle N_{2z}\rangle - x_2\langle N_{1z}\rangle)}{P_t\mathfrak{D}_{12}} - f_{2m}RT\langle N_{2z}\rangle \qquad (30)$$

Summation then leads to the isobaric equation:

$$\left|\frac{\partial P_t}{\partial z}\right| = 0 = -RT(f_{1m}|\langle N_{1z}\rangle| + f_{2m}|\langle N_{2z}\rangle|) \qquad (31)$$

and so the flux ratio is

$$\frac{|\langle N_{1z}\rangle|}{|\langle N_{2z}\rangle|} = -\frac{f_{2m}}{f_{1m}} \qquad (32)$$

which can be written as:

$$\frac{|\langle N_{1z}\rangle|}{|\langle N_{2z}\rangle|} = -\frac{D_1^K + B_0/\kappa_1}{D_2^K + B_0/\kappa_2} = -\frac{\kappa_2}{\kappa_1}\frac{Ke_{2,1} + 1}{Ke_{2,2} + 1} \qquad (33)$$

As is clear from eq 33, in the low limit for $P_t r_0$ (Knudsen region) the flux ratio would approach that of the Knudsen diffusion coefficients and correspond to Graham's law. In the high $P_t r_0$ limit follows:

$$\frac{\langle N_{1z}\rangle}{\langle N_{2z}\rangle} = -\frac{\kappa_2}{\kappa_1} \approx \frac{\eta_2^\circ}{\eta_1^\circ} \qquad (34)$$

It is remarkable that, although molecular diffusion plays a large role here, the ratio of the fluxes is purely determined by wall effects and for the normal region is nearly equal to the ratio of the pure-component viscosities. To my knowledge, this has not been reported before. To illustrate the above relations in Figure 10 for both water−nitrogen and helium−argon, the flux ratio is plotted against the group $P_t r_0$ for a temperature of 298.15 K. For both systems the Graham's law limit at low values of $P_t r_0$ can be observed. For $H_2O-N_2$ at higher values the flux ratio increases, while for He−Ar a slight decrease is observed. This is caused by the pure-component viscosities:

$$\eta_{He} = 2.01 \times 10^{-5}, \quad \eta_{4r} = 2.27 \times 10^{-5},$$
$$\eta_{H_2O} = 1.07 \times 10^{-5}, \quad \eta_{N_2} = 1.76 \times 10^{-5}\ \text{Pa·s}$$

For the porous graphite used by Evans et al. follows a

pore radius $r_0 \approx 3.6 \times 10^{-7}$ m, and at the total pressure of 1.49 bar then follows $P_t r_0 = 0.054$ N/m$^3$. From the graph it can be seen that there is still only a very small deviation from Graham's law at that point. From the analysis it also follows that Graham's law will be found to hold approximately for those systems in which the viscosity ratio is approximately given by:

$$\frac{\eta_2^\circ}{\eta_1^\circ} = \left(\frac{M_2}{M_1}\right)^{1/2} \tag{35}$$

Apparently this is closely approximated for He−Ar, but less so for $H_2O-N_2$.

## 6. The Bosanquet Equation

For equimolar countertransport in a binary gas system generally the Bosanquet equation is given (Froment and Bischoff, 1979):

$$\langle N_{1z}\rangle = -D_{\text{eff},1}\frac{\partial\langle C_1\rangle}{\partial z} \tag{36}$$

$$\frac{1}{D_{\text{eff}}} = \frac{1}{D_{12}} + \frac{1}{D_1^K} \tag{37}$$

From eq 28 of the BFM follows straighforward for $\langle N_{1z}\rangle = -\langle N_{2z}\rangle$:

$$\frac{\partial\langle C_1\rangle}{\partial z} = -\langle N_{1z}\rangle\left(\frac{1}{\text{Đ}_{12}} + f_{1m}\right) = -\langle N_{1z}\rangle\left(\frac{1}{\text{Đ}_{12}} + \frac{1}{D_1^K + \dfrac{B_0}{\kappa_1}}\right) \tag{38}$$

and so indeed in this situation an effective diffusivity can be used:

$$\frac{1}{D_{\text{eff},1}} = \left(\frac{1}{\text{Đ}_{12}} + \frac{1}{D_1^K + \dfrac{B_0}{\kappa_1}}\right) \tag{39}$$

which for high values of the $Ke_2$ number goes over in the Bosanquet equation, and so a typical limit could be:

$$Ke_{2,1} = \frac{D_1^K \kappa_1}{B_0} > 100 \tag{40}$$

For low $Ke_2$ numbers a new equation results:

$$\frac{1}{D_{\text{eff},1}} \approx \left(\frac{1}{\text{Đ}_{12}} + \frac{\kappa_1}{B_0}\right) \tag{41}$$

which shows the effect of viscous wall friction.

## 7. Concluding Remarks

From the foregoing, the usefulness of the binary friction model was demonstrated in considering the Stefan tube and it was shown that it covers a wide range of different regimes. The explicit relation between the wall-friction coefficients and mixture viscosity data allows a quantitative treatment of the problem for all regions which was not availabe before. From the treatment, simple dimensionless numbers were deduced which indicate whether wall-friction or intermolecular friction plays the most important role in the transport, including Knudsen and slip-flow regimes. Also these criteria are new and, moreover, may be extended to other pore transport processes, also for multicomponent systems. From the general BFM equations still an estimate of the importance of wall friction can be made from the criterion:

$$Ke_{1,i} = \frac{f_{im}P_t D_i}{P_t - P_i} = \frac{(P_t D_i)}{\left(D_i^K + \dfrac{B_0}{\kappa_i}\right)P_t(1-x_i)} \approx \frac{(P_t D_i)}{\left(D_i^K + \dfrac{B_0 P_t}{\eta_i^\circ}\right)P_t(1-x_i)} \tag{42}$$

in which $D_i$ is an approximate value of the diffusion coefficient in the mixture. The use of this criterion might greatly facilitate the discussions about the (meso- and macro-) transport in gas adsorption and heterogeneous catalysis, which at present do not have a very clear background (see Kärger and Ruthven, 1992; Froment and Bischoff, 1979; Jackson, 1977) and especially do not include a quantitative aspect of the viscous friction effects, which now are available through the binary friction model. The binary friction model and the criteria here may also be used in estimating the pressure differences within a catalyst particle in the case of nonequimolar reactions.

In the discussion of Graham's law the boundaries were shown, and also it was made clear that in special cases this rule may apply as well outside the Knudsen flow regime, depending on the ratio of the viscosities. The surprising result was found that, at low $Ke_1$ numbers, so in the region in which intermolecular friction is dominating, one may quite accurately estimate the individual fluxes from the simple diffusion equation, but the flux ratio is determined by the ratio of the viscosities.

Also the basis for the Bosanquet equation was extended and the limits of application were derived. For the normal region a new equation was derived.

With all this I have demonstrated that the binary friction model has added clarity to the treatment of basic problems in various chemical engineering areas such as drying, adsorptive separations, and catalytic processes, especially so because it makes various frictional contributions quantitative. The vast area of pore transport problems to which the BFM may be applied offers a fascinating perspective for further study; the simple form of the equations for gases enhances the ease of teaching multicomponent porous transport.

## Acknowledgment

The author wishes to thank one of the reviewers for constructive comments.

## Nomenclature

$A_{\text{capp}}$: cross-sectional area of capillary [m$^2$]
$B_0$: permeability [m$^2$]
$C$: molar concentration [kmol/m$^3$]
Đ: Maxwell−Stefan diffusion coefficient [m$^2$/s]
$D_{\text{eff}}$: effective diffusion coefficient [m$^2$/s]
$D_i^K$: effective Knudsen diffusion coefficient of $i$ [m$^2$/s]
$D_{i0}^K$: zero-pressure Knudsen diffusion coefficient of $i$ [m$^2$/s]
$d_{\text{capp}}$: capillary diameter [m]
$f_{im}$: friction coefficient of component $i$ with wall [s/m$^2$]

$Ke_{1,i}$: wall to interspecies friction ratio for component $i$
$Ke_{2,i}$: Knudsen to viscous friction ratio for component $i$
$L$: capillary length [m]
$M$: molar mass [kg/kmol]
$N$: molar flux vector [kmol/m$^2$ s]
$\langle N \rangle$: cross-section-averaged flux vector [kmol/m$^2$ s]
$|N|$: magnitude of the flux vector [kmol/m$^2$ s]
$N_{DiN}$: Di Napoli number, see eq 24
$P$: pressure [Pa]
$R$: gas constant [J/kmol K]
$r_0$: capillary radius [m]
$T$: absolute temperature [K]
$Wh$: Whitaker number, see eq 26
$x$: mole fraction
$z$: length coordinate [m]

*Greek Letters*

$\phi_{air}$: air stream mixing with outlet vapor [kmol/s]
$\Phi$: formal function, see eq 2
$\eta$: dynamic viscosity [Pa·s]
$\eta_i°$: dynamic viscosity of pure component $i$ [Pa·s]
$\kappa$: fractional viscosity coefficient [s]
$\xi$: Wilke parameter, see eq 11

*Sub- and Superscripts*

1, 2: components
ext: external
$i$, $j$: components
t: total

## Literature Cited


Bird, R. B.; Stewart, W. E.; Lightfoot, E. N. *Transport Phenomena*; John Wiley and Sons: New York, 1960.

Cergignani, C.; Sharipov, F. Gaseous Mixture Slit Flow at Intermediate Knudsen Numbers, *Phys. Fluids A* **1992**, *4*, 1283−1289.

Evans, R. B.; Watson, G. M.; Truitt, J. Interdiffusion of Gases in a Low Permeability Graphite at Uniform Pressure. *J. Appl. Phys.* **1962**, *33*, 2682−2688.

Evans, R. B.; Watson, G. M.; Truitt, J. Interdiffusion of Gases in a Low Permeability Graphite. II. Influence of Pressure Gradients. *J. Appl. Phys.* **1963**, *34*, 2020−2026.

Froment, G. F.; Bischoff, K. B. *Chemical Reactor Analysis and Design*; John Wiley and Sons: New York, 1979.

Jackson, R. *Transport in Porous Catalysts*, Elsevier: Amsterdam, The Netherlands, 1977.

Kärger, J.; Ruthven, D. M. *Diffusion in Zeolites and Other Microporous Systems*; John Wiley and Sons, Inc.: New York, 1992.

Keil, F. J. Modelling of Phenomena within Catalyst Particles. *Chem. Eng. Sci.* **1996**, *10*, 1543−1567.

Kerkhof, P. J. A. M. A Modified Maxwell−Stefan Model for Transport through Inert Membranes: the Binary Friction Model. *Chem. Eng. J.* **1997**, *66*, in press.

Kramers, H. A.; Kistemaker, J. On the Slip of a Diffusing Gas Mixture along a Wall. *Physica X* **1943**, *8*, 699−713.

Krischer, O.; Kast, W. *Die Wissenschaftlichen Grundlagen der Trocknungstechnik, 1er Band*, 3rd ed.; Springer-Verlag: Berlin, 1978.

Lang, H.; Loyalka, S. K. An exact expression for the Diffusion Slip Velocity in a Binary Gas Mixture. *Phys. Fluids* **1970**, *13*, 1871−1873.

Lightfoot, E. N. *Transport in Living Systems*; John Wiley and Sons: New York, 1974.

Mason, E. A.; Viehland, L. A. Statistical−Mechanical Theory of Membrane Transport for Multicomponent Systems: Passive Transport through Open Membranes. *J. Chem. Phys.* **1978**, *68*, 3562−3573.

Mason, E. A.; Malinauskas, A. P. *Gas Transport in Porous Media: The Dusty Gas Model*; Elsevier: Amsterdam, The Netherlands, 1983.

Mason, E. A.; del Castillo, L. F.The Role of Viscous Flow in Theories of Membrane Transport. *J. Membr. Sci.* **1985**, *23*, 199−220.

Mason, E. A.; Lonsdale, H. K. Statistical−Mechanical Theory of Membrane Transport. *J. Membr. Sci.* **1990**, *51*, 1−80.

Mason, E. A.; Malinauskas, A. P.; Evans, R. B., III Flow and Diffusion of Gases in Porous Media. *J. Chem. Phys.* **1967**, *46*, 3199−3216.

Maxwell, J. C. *Scientific Papers, vol. II, p 86*, 1879; in the edition by Niven, W. D. Dover Publications: New York, 1965; pp 681−712.

Mo, G.; Rozenberger, F. Molecular-dynamics Simulations of Flow with Binary Diffusion in a Two-dimensional Channel with Atomically Rough Walls. *Phys. Rev. A* **1991**, *44*, 4978−4985.

Noever, D. A. The Baroeffect and an Appropriate Momentum Boundary Condition. *Phys. Fluids A* **1990**, *5*, 858−865.

Reid, R. C.; Prausnitz, J. M.; Sherwood, T. K. *The Properties of Gases and Liquids*; McGraw-Hill: New York, 1977.

Robertson, B. C.; Zydney, A. L. Stefan−Maxwell Analysis of Protein Transport in Porous Membranes. *Sep. Sci. Technol.* **1988**, *23*, 1799−1811.

Veldsink, J. W.; van Damme, R. M. J.; Versteeg, G. F.; van Swaaij, W. P. M. The Use of the Dusty-Gas Model for the Description of Mass Transport with Chemical Reaction. *Chem. Eng. J.* **1995**, *57*, 115−125.

Waldmann, L.; Schmitt, K. H. Über das bei der Gasdiffusion auftretende Druckgefälle. *Z. Naturforsch.* **1961**, *16A*, 1343−1354.

Whitaker, S. Levels of Simplification: The Use of Assumptions, Restrictions and Constraints in Engineering Analysis. *Chem. Eng. Ed.* **1988**, *22*, 104−108.

Whitaker, S. The Development of Fluid Mechanics in Chemical Engineering. *One Hundred Years of Chemical Engineering*; In Peppas, N., Ed.; Kluwer Academic Publishers: Dordrecht, The Netherlands, 1989; pp 45−109.

Whitaker, S. Role of the Species Momentum Equation in the Analysis of the Stefan Diffusion Tube. *Ind. Eng. Chem. Res.* **1991**, *30*, 978−983.


*Received for review* September 3, 1996
*Revised manuscript received* November 14, 1996
*Accepted* November 21, 1996[⊗]

IE960542I

[⊗] Abstract published in *Advance ACS Abstracts*, January 15, 1997.